Approximate Molecular Electrostatic Potentials from Semiempirical Wavefunctions

MATTHIAS KRACK, ANDREAS M. KÖSTER, KARL JUG*

Theoretische Chemie, Universität Hannover, Am Kleinen Felde 30, 30167 Hannover, Germany

Received 8 May 1995; revised 17 October 1995

ABSTRACT: Approximate molecular electrostatic potentials (MESPs) are calculated with the asymptotic density model (ADM) on the basis of semiempirical wavefunctions generated by the SINDO1 method. The approximate MESP is adjusted to obtain good agreement with the exact MESP from 6-31G* *ab initio* calculations for small molecules. This form of the MESP is used for the study of the reactivity of small and medium size silicon clusters with 5 to 45 atoms. Special attention is given to the reactivity of various Si_{45} structures proposed in the literature. © 1997 by John Wiley & Sons, Inc.

Introduction

The molecular electrostatic potential (MESP) is a physical observable which is particularly suitable for the study of reactivity of molecules. The MESP allows to identify the site of a molecule where a nucleophilic or an electrophilic attack will preferably take place. For the representation of the MESP, its value has to be calculated in general at each point of a two- or three-dimensional grid. Depending on symmetry, only a two-dimensional grid may be needed for small molecules. Such two-dimensional contour plots already give a good picture of the MESP of a molecule so that calculations of the MESP are needed at only a few thousand points. For larger systems or systems with low symmetry, it is necessary to represent the MESP in three-dimensional form on a surface around the molecule, in order to have a suitable view of the site of attack by a nucleophile or electrophile. There are two problems connected with the three-dimensional representation: The choice of the surface and the numbers of grid points on the surface for the MESP. The latter is a technical problem which can be solved by choosing a few ten thousands of points for large molecules. The former problem is more fundamental because the choice of the surface for the MESP significantly influences the qualitative statement on the reactivity of a system. If the surface for the MESP calculation is too close to the nuclei, then the MESP on this surface is highly positive due to

*Author to whom all correspondence should be addressed.

CCC 0192-8651 / 97 / 18, No. 3, 301–312 (1997)

Keywords: 030301-12

the dominating positive potential of the nuclei. In this case it is not possible to distinguish between nucleophilic or electrophilic reactivity. A similar argument is valid for a molecular surface, which is too far away from the nuclei, because the value of the MESP approaches zero for large distances. Therefore, the MESP on such a molecular surface does not produce the necessary contours for the reactivity description.

To solve the technical problem, attempts have been made to speed up the exact calculation of the MESP by algorithmic improvements.[1] For larger systems, the exact calculation is still rather computer time consuming. Another possibility is the approximation of the MESP. For this purpose we have developed the asymptotic density model (ADM).[2] Here the asymptotic behavior of the density at the atomic nuclei and for large distances from the nuclei is correctly accounted for in the density approximation. The approximation of the MESP by the ADM on the basis of an *ab initio* wavefunction gave very good results in comparison with the exact MESP. The approximate calculation of the MESP by the ADM is much faster than the exact calculation, because only simple analytical expressions have to be evaluated. This is particularly efficient for very large systems. However, in this case, *ab initio* calculations are not feasible. It is therefore suggestive to use semiempirical instead of *ab initio* wavefunctions, even if there is some loss of quality in the wavefunction. We have therefore tried to develop a successful combination of two approximate methods, namely the ADM and the SINDO1 methods.

The Aymptotic Density Model

The electrostatic potential $U(\mathbf{r})$ at a position $\mathbf{r}$ is the sum of a nuclear contribution $U_{\text{nuc}}(\mathbf{r})$ and an electronic contribution $U_{\text{el}}(\mathbf{r})$. In MO theory these can be formulated as

$$\begin{aligned} U(\mathbf{r}) &= U_{\text{nuc}}(\mathbf{r}) + U_{\text{el}}(\mathbf{r}) \\ &= \sum_A \frac{Z_A}{|\mathbf{R}_A - \mathbf{r}|} - \int \frac{\rho(\mathbf{r}')}{|\mathbf{r}' - \mathbf{r}|} d\mathbf{r}' \\ &= \sum_A \frac{Z_A}{|\mathbf{R}_A - \mathbf{r}|} - \sum_{a,b} P_{a,b} \left\langle \chi_a \left| \frac{1}{|\mathbf{r}' - \mathbf{r}|} \right| \chi_b \right\rangle \end{aligned} \quad (1)$$

Here Z_A is the nuclear charge of atom A, $\rho(\mathbf{r}')$ the density at $\mathbf{r}'$, $\mathbf{R}_A$ the position vector of A, and P_{ab} a density matrix element. The contribution of the nuclei can be easily calculated. In contrast, the electronic portion is more complicated, because it requires the calculation of one-, two-, and three-center core attraction integrals. A three-center core attraction appears from the last term in eq. (1) if χ_a is on atom A, χ_b on atom B and the inverse distance operator is from atom C. To avoid these complications, in particular from the difficulty of calculation and number of the three-center integrals, we use the ADM as a suitable approximation. A detailed derivation of the ADM for *ab initio* wavefunctions was published previously.[2] Here we shall give only a brief description necessary for the basic understanding of the method. In the asymptotic density model the total density was expanded in atomic densities

$$\rho_M(\mathbf{r}) = \sum_A^M \rho_A(\mathbf{R}_A + \mathbf{r}_A) \quad (2)$$

In a local coordinate system we put the position vector $\mathbf{R}_A$ of atom A equal to zero. Since the density of a single atom is a monotonically decreasing function of the distance, it can be approximated by a superposition of exponential functions.[3] In the framework of the modified ADM the for semiempirical wavefunctions following form of the density $\rho(r, \vartheta, \varphi)$ was taken

$$\begin{aligned} \rho(\mathbf{r}_A) = {} & c_{00} e^{-\alpha_{00} r_A} S_{00}(\vartheta_A, \varphi_A) \\ & + \sum_{m=-1}^{1} c_{1m} r_A e^{-\alpha_{1m} r_A} S_{1m}(\vartheta_A, \varphi_A) \end{aligned} \quad (3)$$

The first exponential function describes the spherical part of the density. The factor c_{00} is determined by the atomic charge. The other three exponential functions serve to generate a polarization of the atomic density along the Cartesian axes and thus allow a description of anisotropy of the atomic density. The factor c_{1m} are determined by atomic dipole moments. The S_{lm} are spherical harmonics in real form. The procedure for solution is the following. The approximation (3) is introduced into the Poisson equation

$$\nabla^2 U_A(\mathbf{r}_A) = -4\pi\rho_A(\mathbf{r}_A) \quad (4)$$

which is subsequently solved for each U. The $U_A(\mathbf{r}_A)$ are expanded in terms depending on l and m

$$U_A(\mathbf{r}_A) = \sum_{l,m} U_{lm}^A(\mathbf{r}_A) \quad (5)$$

Each U_{lm}^A consists of a homogeneous and an inhomogeneous solution of the Poission equation

$$U_{lm}^A(\mathbf{r}_A) = U_{lm}^{A,\,\mathrm{hom}}(\mathbf{r}_A) + U_{lm}^{A,\,\mathrm{inhom}}(\mathbf{r}_A) \quad (6)$$

The homogeneous part is given by the multipole expansion

$$U_{lm}^{A,\,\mathrm{hom}}(\mathbf{r}_A) = \frac{4\pi}{2l+1} q_{lm}^A r_A^{-l-1} S_{lm}(\vartheta_A, \varphi_A) \quad (7)$$

Here we need only the atomic charges Q_0 and the cumulative Cartesian atomic dipole components Q_x, Q_y, Q_z to define

$$q_{00} = \sqrt{\frac{1}{4\pi}}\, Q_0, \quad q_{10} = \sqrt{\frac{3}{4\pi}}\, f_A Q_z,$$
$$q_{11} = \sqrt{\frac{3}{4\pi}}\, f_A Q_x, \quad q_{1-1} = \sqrt{\frac{3}{4\pi}}\, f_A Q_y \quad (8)$$

f_A is an atomic parameter to adjust the approximate MESP to the exact MESP from an *ab initio* calculation. Due to the form of (3) we obtain a spherical part U_0^A and a nonspherical part U_1^A, which are sums of homogeneous and inhomogeneous solutions.

$$U_0^A = 4\pi \left[\frac{1}{r_A} - \left(\frac{1}{r_A} + \frac{\alpha_{00}}{2} \right) e^{-\alpha_{00} r_A} \right] q_{00}^A S_{00}(\vartheta_A, \varphi_A) \quad (9)$$

$$U_1^A = \frac{4}{3}\pi \left[\frac{1}{r_A^2} - \left(\frac{1}{r_A^2} + \frac{\alpha_{1m}}{r_A} + \frac{\alpha_{1m}^2}{2} + \frac{\alpha_{1m}^3 r_A}{8} \right) \times e^{-\alpha_{1m} r_A} \right] \sum_{m=-1}^{1} q_{1m}^A S_{1m}(\vartheta_A, \varphi_A) \quad (10)$$

Due to the neglect of the contribution of the electrons of the other atoms to the MESP at atom A the following scaling is necessary

$$\lim_{\mathbf{r}_A \to 0} U_A(\mathbf{r}_A) = \alpha'_{00} U_{\mathrm{el}}^{\mathrm{exact}}(\mathbf{r}_A) \quad (11)$$

α_{00} is related to α'_{00} by

$$\alpha_{00} = \frac{\alpha'_{00} U_{\mathrm{el}}^{\mathrm{exact}}}{2\pi q_{00} S_{00}} \quad (12)$$

The cumulative atomic multipole moments (CAMM)[4,5] are defined in such a way that the rotational invariance of all moments is preserved. In a nonorthogonal basis, the cumulative charge and dipole moment of atom A are represented by the following expressions

$$Q_0^A = Z_A - \sum_a^A \sum_b P_{ab} S_{ab} \quad (13)$$

$$Q_z^A = \sum_a^A \sum_b P_{ab}(S_{ab} z_A - z_{ab})$$
$$\text{with } z_{ab} = \langle \chi_a |\, z \,| \chi_b \rangle \quad (14)$$

z represents one of the three components of the dipole moment. In a symmetrically orthogonalized basis λ[6] similar expression are obtained

$$Q_0^A = Z_A - \sum_a^A P_{aa}^\lambda \quad (15)$$

$$Q_z^A = \sum_{\mathrm{a}}^{\mathrm{A}} \sum_{\mathrm{b}} P_{ab}^\lambda(\delta_{\mathrm{ab}} z_A - z_{ab})$$
$$\text{with } z_{ab} = \langle \lambda_a | z | \lambda_b \rangle \quad (16)$$

The approximate MESP at point $\mathbf{r}$ is finally given as the sum over all atoms

$$U_{\mathrm{nuc}}(\mathbf{r}) = \sum_A \frac{Z_A}{|\mathbf{R}_A - \mathbf{r}|} \quad (17)$$

$$U_{\mathrm{el}}(\mathbf{r}) = \sum_A (U_0^A(\mathbf{r}) + U_1^A(\mathbf{r})) \quad (18)$$

Implementation of ADM in SINDO1

Our intention was to incorporate the idea of the ADM into a semiempirical method. We have chosen SINDO1 because this method was developed in our laboratory, but an implementation in other semiempirical methods is also possible with minor modifications. SINDO1[7–10] is a semiempirical SCF MO method based on the INDO approximation in a minimal basis set of Slater orbitals (STOs). The symmetrical orthogonalization of the basis reduces the error introduced by the neglect of differential overlap. Due to the INDO approximation and justified by the symmetric orthogonalization no two-center dipole integrals were retained. For the calculation of the cumulative atomic dipole moments the complete dipole integral matrices over nonorthogonal STOs are needed. For the calculation of the missing integrals an integral program was developed which could be easily incorporated as a subroutine into SINDO1. This program calculates overlap, core attraction, and dipole integrals over STOs for a general spd basis set up to quan-

tum number $n = 4$ in a local coordinate system. The integral matrices are then transformed from the local to the global coordinate system by suitable transformation matrices. The core attraction integrals are needed for the calculation of the electrostatic potential U_{el}^{exact} at atom A. The overlap integrals are programmed for control purposes. All integrals were solved in elliptic coordinates and expanded in auxiliary functions. The resulting formulas were explicitly programmed and can be effectively accessed by tabular address. For the integral table the address is calculated from the quantum numbers of the corresponding STOs. Most of the computer time is used for the transformation of the local into the global coordinate system, whereas the integral calculation needs relatively little computer time.

The density matrix $\mathbf{P}^{\lambda}$ in the symmetrically orthogonalized basis and the overlap matrix $\mathbf{S}$ are generated by the SINDO1 program. The dipole matrices $\mathbf{X}$, $\mathbf{Y}$ and $\mathbf{Z}$ are calculated in a nonorthogonal STO basis.

There are two ways to calculate the molecular dipole moments. In the symmetrically orthogonalized basis the dipole matrices must be transformed as

$$\mathbf{U}^{\lambda} = \mathbf{S}^{-1/2}\mathbf{U}\mathbf{S}^{-1/2} \tag{19}$$

where $\mathbf{U}$ is one of the three dipole matrices. From $\mathbf{X}^{\lambda}$, $\mathbf{Y}^{\lambda}$, and $\mathbf{Z}^{\lambda}$ together with $\mathbf{P}^{\lambda}$ the dipole moments can be calculated. Alternatively, the density matrix $\mathbf{P}^{\lambda}$ can be transformed to a matrix $\mathbf{P}$ in a nonorthogonal basis set

$$\mathbf{P} = \mathbf{S}^{-1/2}\mathbf{P}^{\lambda}\mathbf{S}^{-1/2} \tag{20}$$

We have chosen the second way, because in this case only one instead of three matrices have to be transformed.

The use of the exact $\mathbf{S}^{-1/2}$ matrix did not lead to satisfactory results for the dipole moments within the model adjustment. We attributed this to the fact that in SINDO1 the $\mathbf{S}^{-1/2}$ matrix was replaced by a truncated binomial expansion of the form

$$\mathbf{S}^{-1/2} = (\mathbf{1} + \boldsymbol{\sigma})^{-1/2} = \mathbf{1} - \tfrac{1}{2}\boldsymbol{\sigma} + \tfrac{3}{16}\boldsymbol{\sigma}^2 \tag{21}$$

The constant factor is here $\frac{3}{16}$ instead of $\frac{3}{8}$ to take the truncation into account. In consequence, we use this expansion also in the back transformation. The density matrix $\mathbf{P}$ can be used for a Mulliken population analysis. Here the factor $\frac{3}{16}$ also proves to be better than $\frac{3}{8}$. This procedure worked for H and the elements of the first row from Li to F. In the second row the charges for silicon turned out to be too large. Therefore all matrix elements σ_{ab} with a on atom A and b on atom B were scaled

$$\sigma'_{ab} = k_A \sigma_{ab} k_B \tag{22}$$

For hydrogen and for the elements of the first row from Li to F no scaling of $\boldsymbol{\sigma}$ is necessary. For these elements k is set equal to 1.0. For silicon $k_{Si} = 0.90$ resulted in satisfactory charges. Other elements of the second and third row have not yet been parametrized with respect to k. In the following we present a comprehensive description of the MESP calculation with SINDO1 using the ADM. The SINDO1 density matrix $\mathbf{P}^{\lambda}$ is transformed according to eqs. (20)-(22). The resulting P_{ab} values are used to compute the cumulative atomic charge and dipole moments Q_0 and Q_x, Q_y, Q_z in eq. (8). The potentials U_0^A and U_1^A are calculated using eq. (9) and (10). The MESP value at point $\mathbf{r}$ is computed according to eq. (1) after introducing eqs. (17) and (18). The back transformation of the density matrix and the parameters f_A of eq. (8) and k_A of eq. (22) are specific for SINDO1. However, the ADM can be implemented also in other semiempirical methods, because only the density matrix, the overlap matrix, and the dipole integral matrices are needed. The fitting of parameters must be performed separately for each semiempirical method.

The time for the MESP calculation using several 10,000 grid points is small compared to the time needed to generate the density matrix. Our model uses analytical expressions for the MESP calculation in the framework of the ADM. Another fast method is the multicenter point charge model of Rauhut and Clark[11] where hybrid charges are used beside the core charges. Our method is superior to the method described by Reynolds et al.[12] where semiempirical electrostatic potentials are derived only for the outer regions of molecules.

Parametrization of Dipole Moments

Before the approximate electrostatic potentials could be generated, the dipole moments had to be parametrized. The atomic parameters f_A in eq. (8) serve for the scaling of dipole moments. In Table I the values for f_A are listed together with those for

TABLE I.
Atomic Parameters for the Calculation of Dipole Moments

Parameter	H	Li	B	C	N	O	F	Si
f_A	0.8	1.0	1.1	1.0	1.3	1.4	1.6	1.2
k_A	1.0	1.0	1.0	1.0	1.0	1.0	1.0	0.9

k_A for the back transformation. Table II lists the new dipole moments calculated with these parameters together with the old values and with the experimental values.[13,14] There is a slight improvement in the average error from 0.35 Debye in the old version to 0.30 Debye in the new version. Altogether the dipole moments depend on the quality of the SINDO1 wavefunction. If the charge distribution in a molecule is not well represented or the calculated SINDO1 geometry is not good, the exact dipole matrices cannot eliminate this deficiency. It is remarkable that there is an improvement in molecules like ammonia or hydrogen fluoride which are well represented by SINDO1 with respect to charge and geometry. Obviously the hybrid moments play a significant role in these molecules. For a molecule like N_2O correlation effects are important. Part of the correlation is usually included in the ground-state parametrization of a semiempirical method. For N_2O this parametrization is insufficient. But a few configurations in a configuration interaction (CI) calculation suffice to improve the SINDO1 dipole moment of N_2O.

TABLE II.
Dipole Moments (Debye)

	SINDO1			Deviation	
Molecule	New	Old	Experiment[a]	New	Old
BF	0.56	0.76	0.50	0.06	0.26
BH	1.56	1.61	1.27	0.29	0.34
BHF_2	1.47	1.06	0.97	0.50	0.09
BNH_6	5.05	6.21	5.05	0.00	1.16
CF_2O	0.19	0.65	0.95	−0.76	−0.30
CH_2F_2	2.12	1.78	1.96	0.16	−0.18
CH_2O	1.72	1.53	2.17	−0.45	−0.64
CH_3F	1.78	1.59	1.85	−0.07	−0.26
CHF_3	1.79	1.51	1.65	0.14	−0.14
CHFO	1.91	1.66	2.02	−0.11	−0.36
CO	0.13	0.57	0.15	−0.02	0.42
HCN	2.21	2.35	2.96	−0.75	−0.61
HF	1.61	1.49	1.69	−0.08	−0.20
HOF	1.93	1.55	2.23	−0.30	−0.68
H_2O	1.75	1.94	1.84	−0.09	0.10
LiF	6.44	6.01	6.28	0.16	−0.27
LiH	5.64	5.75	5.70	−0.06	0.05
NF_3	0.74	0.20	0.21	0.53	−0.01
NH_3	1.69	2.20	1.47	0.22	0.73
NHF_2	1.97	1.57	1.92	0.05	−0.35
^2NO	0.10	0.01	0.15	−0.05	−0.14
$^2NO_2$	1.03	0.60	0.32	0.71	0.28
N_2O	1.46	0.93	0.16	1.30	0.77
OF_2	0.58	0.25	0.18	0.40	0.07

[a] Refs. 13 and 14

Parametrization of the Asymptotic Density Model

Figures 1 to 5 show the contour plots of the MESP for HF, LiH, LiF, H_2O, and Si_5. For comparison the exact MESP from a 6-31G* *ab initio* calculation with Gaussian 90[15] is also presented. On inspection we see that the agreement between the approximate and the exact MESP is very satisfactory. For ionic compounds like LiF the differences are very small. For the parametrization of the depicted MESP contour plots the parameters α'_{00} and α_{1m} were used. The parameters were not automatically optimized, but by a stepwise procedure during which the visual impression of similarity with the exact MESP was the criterion. This parameter optimization had already been successfully applied in the adjustment of the parameters on the basis of an *ab initio* wavefunction. The resulting parameters are in Table III.

The Molecular Surface

The three-dimensional representation of the MESP on a molecular surface allows also a comparison of reactivity for larger structures. In our reactivity study for silicon clusters,[16] we have considered different kinds of molecular surfaces. The simplest way to generate a surface is from rigid spheres around each atom. For the sphere radii, scaled van der Waals radii are used for each element. A weakness of this kind of surface are the unrealistic cusps at the intersection of the spheres in the bonding region between two atoms. A better surface is obtained by the motion of a sphere on such a van der Waals surface[17,18] which smooths out these cusps. To generate such surfaces the program GEPOL[19] was implemented in SINDO1. GEPOL produces various surfaces used in the literature in the form of a point grid. For each grid point the MESP is calculated with ADM.

All these surfaces have one weakness in common: they use rigid spheres with more or less arbitrary sphere radii which do not take into account the different chemical environment of atoms in molecules. A better choice seems to be an isodensity surface because it also contains information on the electronic structure of a molecule. We have therefore chosen isodensity surfaces in this study. However, the choice of the limiting density value is initially arbitrary. Murray and Politzer[20] and Brinck et al.[21] have used in their numerous studies density values of 0.001 or 0.002 electrons/Bohr^3. In our density studies we have

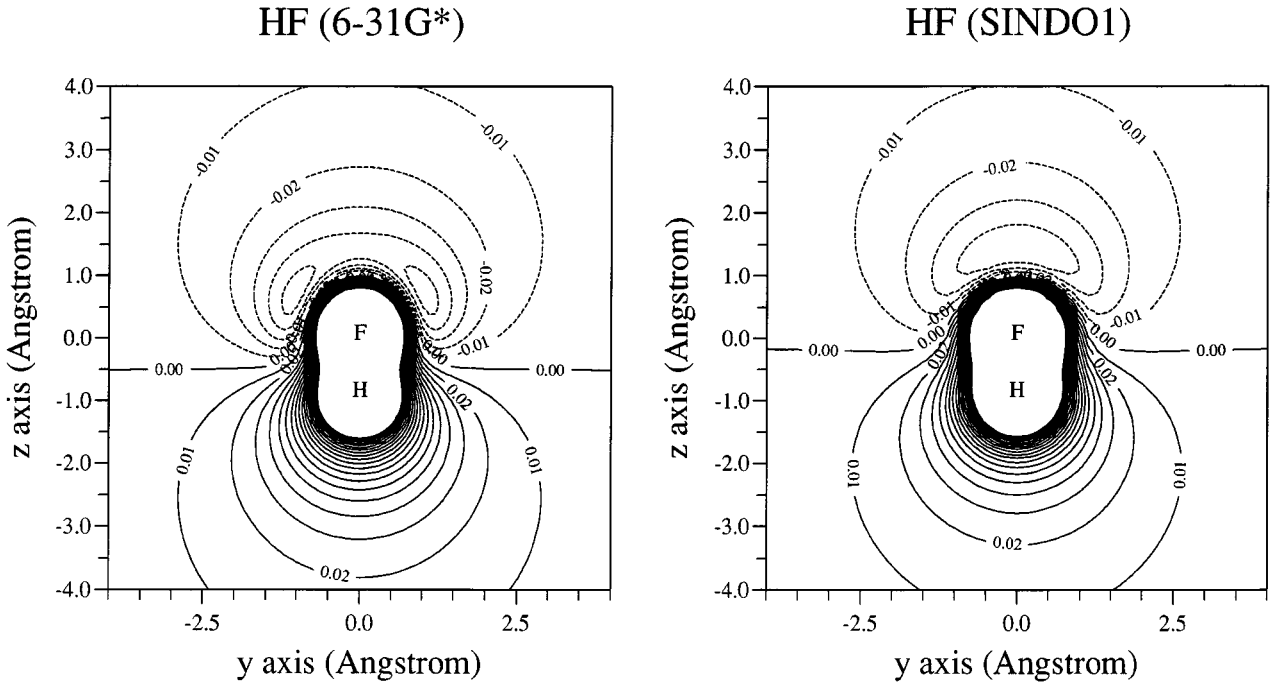

FIGURE 1. MESP contour plot (a.u.) of HF.

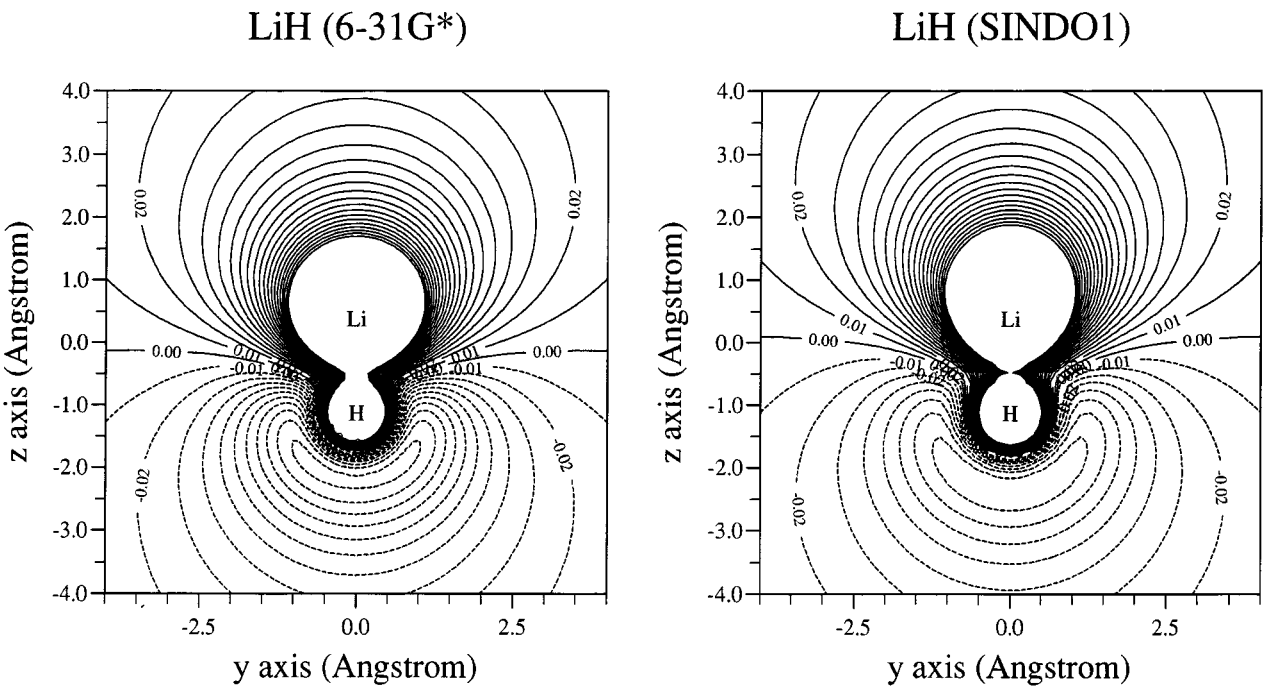

FIGURE 2. MESP contour plot (a.u.) of LiH.

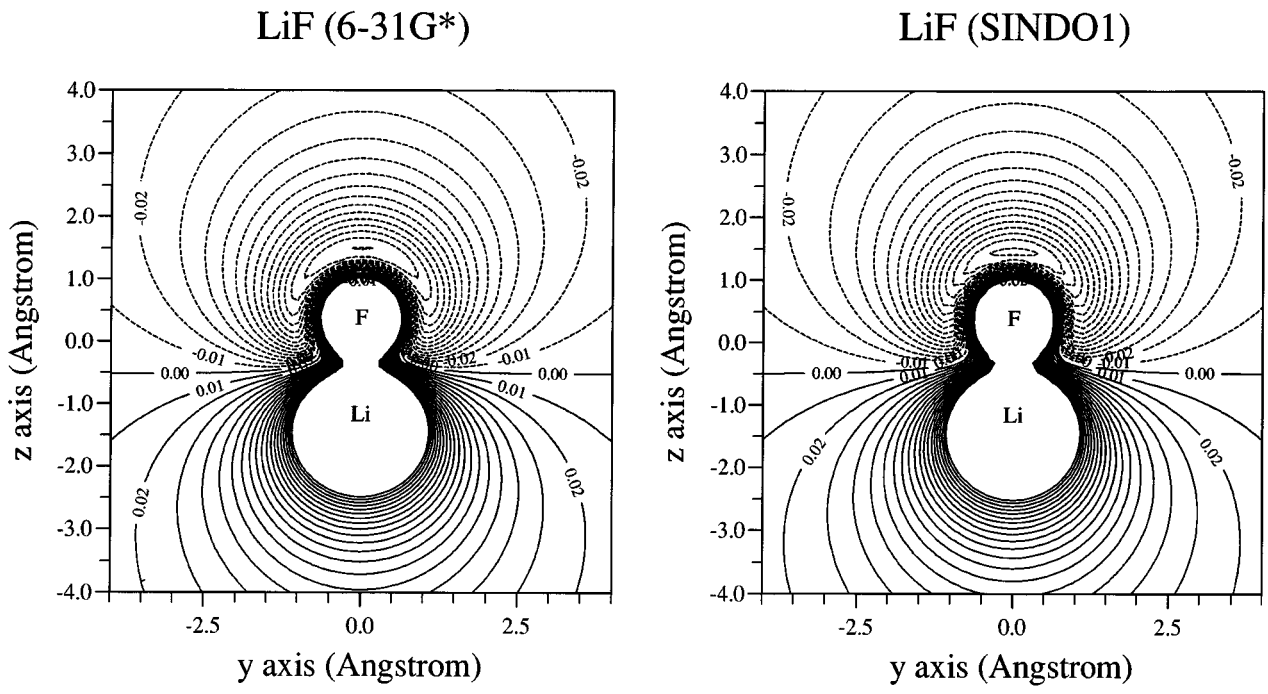

FIGURE 3. MESP contour plot (a.u.) of LiF.

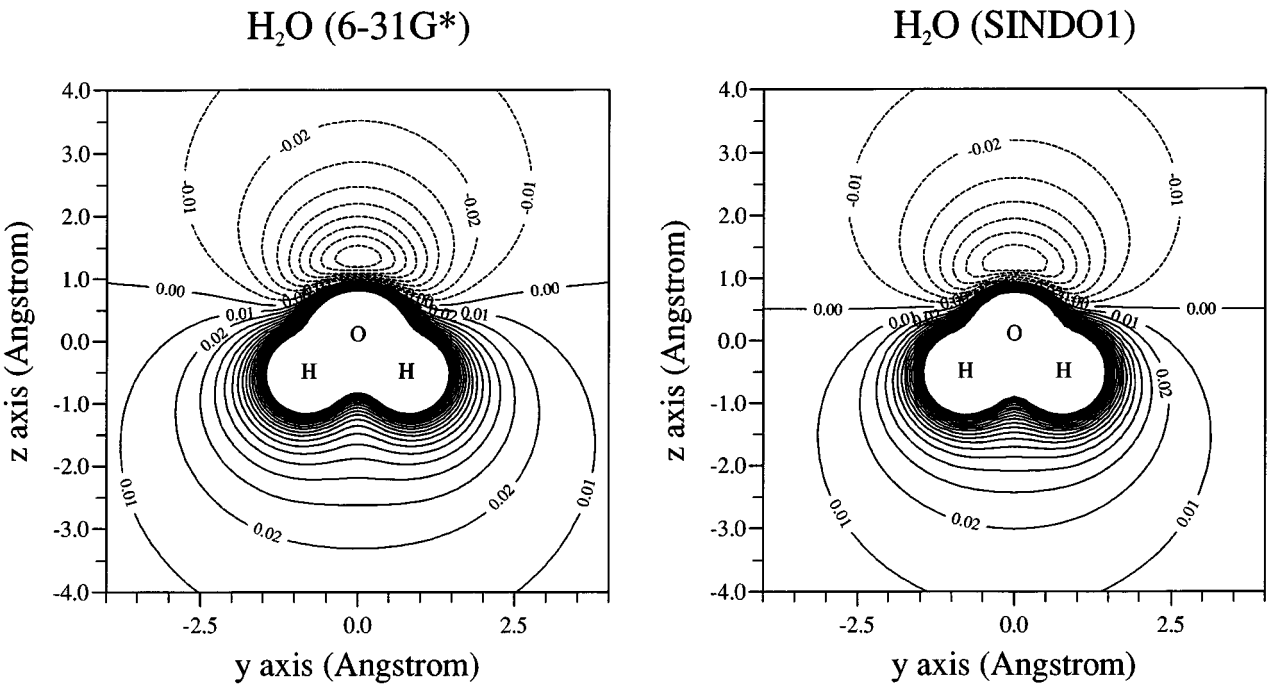

FIGURE 4. MESP contour plot (a.u.) of H_2O.

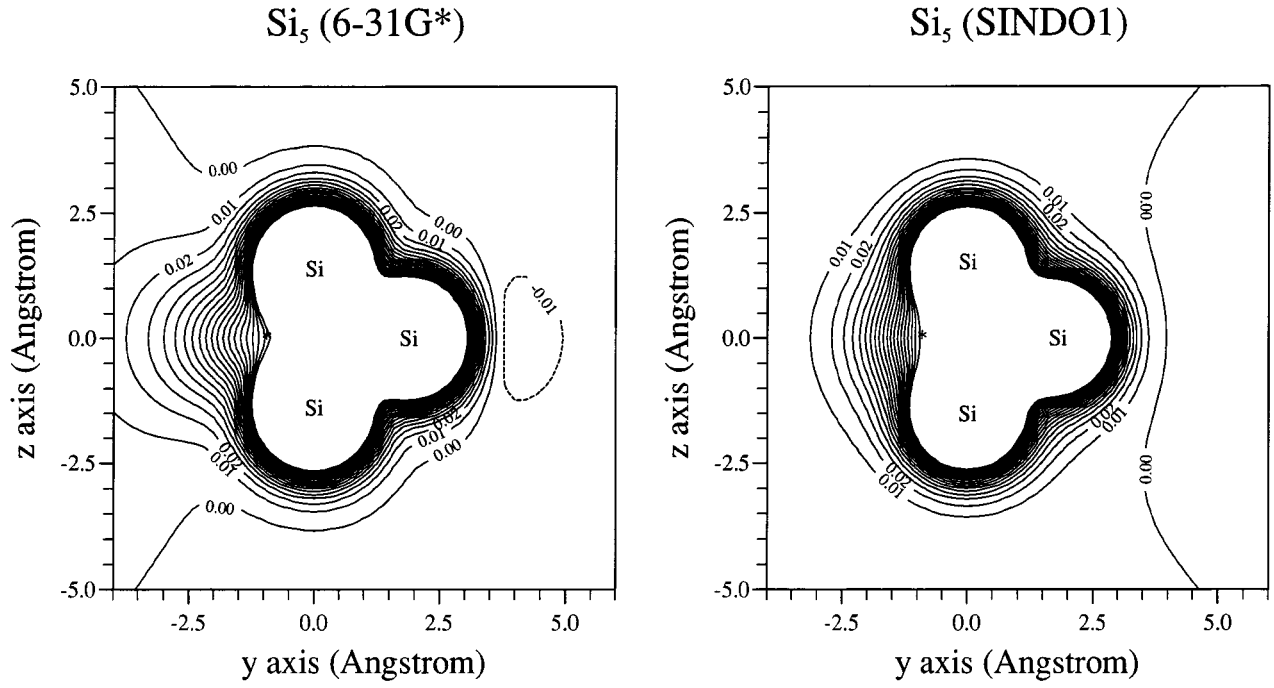

FIGURE 5. MESP contour plot (a.u.) of Si_5.

TABLE III.
Atomic Parameters for the Calculation of the MESP

Parameter	H	Li	B	C	N	O	F	Si
α'_{00}	0.8	1.5	1.6	1.6	1.8	1.4	1.2	1.7
α_{1m}	0.8	1.5	1.6	1.6	1.8	1.4	1.2	2.5

chosen 0.001 electrons/Bohr^3. Such an isodensity surface encloses more than 95% of the density of a molecule.[22] The choice of a reasonable isodensity value is decisive for a qualitative assertion of the reactivity. For a comparison of the MESP of different systems it is therefore necessary to use the same isodensity value.

For the generation of an isodensity surface, the electronic density was calculated at all points of a three-dimensional grid according to the ADM approach of eqs. (2) and (3). In this way the MESP and the electronic density correspond consistently on the basis of the ADM. Also a quick calculation of the density is possible. The isodensity surface is then built up with the aid of the marching cube algorithm.[23, 24]

Reactivity of Silicon Clusters

After the successful application of the ADM to the MESP of the small molecules we now present systems which are not easily accessible to *ab initio* methods. We have used SINDO1 with the implemented ADM for the following studies. As a first application the reactivity of silicon clusters with 5, 10, and 45 atoms was investigated with the MESP. In Figures 6a and 6b the most stable structural isomers of Si_5 and Si_{10} are represented. The Si_5 cluster is a trigonal bipyramid. The Si_{10} cluster is a fourfold alternatingly capped octahedron. In 6-31G* calculations[26, 27] these two structures were also the most stable structural isomers. From the MESP contour plot in Figure 5 one already can see that the zero line bypasses atoms 1, 2, and 3. This means that there is a weak negative MESP at these atoms which make a nucleophilic attack at these atoms unfavorable. This result agrees with our explicit potential curve calculations for the NH_3/Si_5 system.[16] Here ammonia approaches atoms 1 and 5 of the Si_5 cluster as a nucleophile. The interpolation of the N-Si distance yielded two potential curves, but only the curve for atom 5 showed a minimum. The evaluation of the CAMMs had already resulted in a qualitatively correct description of the reactivity, whereas the sole evaluation of the net charges had led to a wrong conclusion about the reactivity. The exact picture of the MESP shows an even more negative MESP at atoms 1, 2, and 3. Here the zero line bypasses also atoms 4 and 5 of the Si_5 cluster. The qualitative conclusion is, however, unchanged, because atoms 4 and 5 are still favored in a nucleophilic attack.

The three-dimensional representation of the MESP for the Si_5 cluster in Figure 7a allows an even better assessment of the reactivity than a contour plot. From the dark green color one recognizes a weakly negative potential for atoms 1, 2, and 3 of the Si_5 cluster, whereas a weakly positive potential is indicated for atoms 4 and 5 by the light green color. This means that atoms 4 and 5 are favored in a nucleophilic attack, whereas atoms 1, 2, and 3 are favored in an electrophilic attack.

There is a similar picture for the Si_{10} cluster. The four capping atoms (7–10) of the octahedron (Fig. 7b) show a dark green color. An electrophilic attack should therefore occur at these atoms. The atoms (1–6) of the octahedron show a positive potential favoring a nucleophilic attack. The explicit calculations have shown that the adsorption energies atoms 1–6 and 7–10 differ by less than 3 kcal/mol.

The MESP near atoms 1–3 of Si_5 and 7–10 of Si_{10} is very similar and the same is found for atoms 4–5 of Si_5 and 1–6 of Si_{10}, respectively. Hence, both clusters are predicted to have low reactivity in electrophilic and nucleophilic attacks in this electrostatic model. However, an explicit calculation for the Si_5 cluster resulted in a significant difference for the adsorption energies at atoms 1 and 4 due to local relaxation. This latter effect is not accounted for in the simple reactivity model.

This local relaxation is less important in larger cluster structures where there is a more pronounced difference in the MESP of different atoms.

The surfaces of the Si_5 and Si_{10} cluster have a positive potential. Therefore, the first attack of a nucleophile will be in the direction of these surfaces. But since ammonia cannot bind to a surface as the explicit calculations have shown, the nitrogen atom of ammonia will eventually bind to an atom which is close by. Thus only the MESP in the neighborhood of the surface atoms is relevant for the reactivity toward ammonia. A particularly low reactivity toward ammonia was measured for the cation of the Si_{45} cluster.[28,29] Since then several structures for the Si_{45} cluster have been proposed in the literature. At first there was a search for energetically stable structures. However, pronounced energetic stability of a structure does not imply low reactivity toward ammonia. Therefore the corresponding Si_{45} structures were optimized with SINDO1 and the MESP approximated by the ADM was plotted on an isodensity surface of 0.001 electrons/Bohr^3 around the clusters. The relative stabilities of the clusters were previously presented.[30] Since all cluster structures have a high symmetry (T or T_d), a representation from one side suffices to get a good total impression of the MESP. Figure 6c shows the structure of Kaxiras,[31], Figure 7c the contour plot corresponding to Figure 6c. On the surface of Figure 7c, one can see zigzag chains of surface atoms which show a dark green, negative MESP. These chains were already described by Kaxiras as so-called π chains. Three of these chains (16-28-39-15, 18-30-34-12, and 11-23-38-14) can be seen in Figure 7c. Atoms 26, 36, and 40 show a weakly positive MESP. A highly positive MESP is at atom 2 which is located on the C_3 axis of the cluster. The pink color shows that the value of the MESP surpasses the upper limit of the scale. For symmetry reasons there are three further atoms with the same MESP. These atoms would be reactive centers for a nucleophilic attack. Also the Si_{45} structure of Patterson and Messmer[32] (Figure 8a) shows four highly positive atoms including atom 2 (Fig. 9a). The eight four-membered rings on the surface have a negative MESP. In contrast, atoms 12, 13, and 14 have a slightly positive MESP. The Si_{45} cluster of Jelski et al.[33] (Figure 8b) has certainly four six-membered rings of atoms with a negative MESP, but each ring is capped with an atom which has a positive MESP around it, e.g., atom 33 (Fig. 9b). These atoms are ideal positions for a nucleophilic attack, because they are sufficiently exposed for an attacking molecule. Atom 10 has an even more positive MESP, but is less exposed, and provides another site for nucleophilic attack. Our proposed structure (Fig. 8c) for Si_{45} cluster[30] shows also a distinctly positive MESP (Fig 9c). However, the red color rather than the pink color indicates a smaller positive MESP value than for the other structures. Atoms 12, 13, and 14 have a slightly positive MESP indicated by the yellow color.

Conclusions

The application of the ADM on the basis of semiempirical wavefunctions allows the study of the reactivity with the MESP also for relatively large structures. The time for the MESP calculation using several ten thousand grid points is small compared to the time needed to generate the density matrix, because the MESP calculation in the framework of the ADM is based on simple analytical formulas. The ADM can be implemented also in other semiempirical methods, because only the density matrix, the overlap matrix, and the dipole integral matrices are needed. Each of the presented Si_{45} structures possesses several atoms with a pronounced positive MESP on the surface. It is interesting that there is a negative MESP on the surface close to the exposed atoms, whereas the lower lying surface atoms on the C_3 axes have a pronounced positive MESP. Despite the difference in structure we find here interesting similarities which may be helpful. The Si_5 cluster is the least reactive. The Si_{10} cluster is also little reactive compared to the Si_{45} clusters. Obviously the reactivity increases with increasing cluster size, which agrees with observations from experiment.[28] This conclusion has to be supported by an investigation of larger silicon cluster structures. In the comparison

FIGURE 6. Structure of a) Si_5 (D_{3h}), b) Si_{10} (T_d), c) Si_{45} (T)[31].
FIGURE 7. MESP (a.u.) on an isodensity surface (0.001 e/Bohr^3) around. (a) Si_5 (D_{3h}), (b) Si_{10} (T_d), (c) Si_{45} (T)[31].
FIGURE 8. Structure of a) Si_{45} (T_d)[32], b) Si_{45} (T_d)[33], c) Si_{45} (T_d)[30].
FIGURE 9. MESP (a.u.) on an isodensity surface (0.001 e/Bohr^3) around. (a) Si_{45} (T_d)[32], (b) Si_{45} (T_d)[33], (c) Si_{45} (T_d)[30].

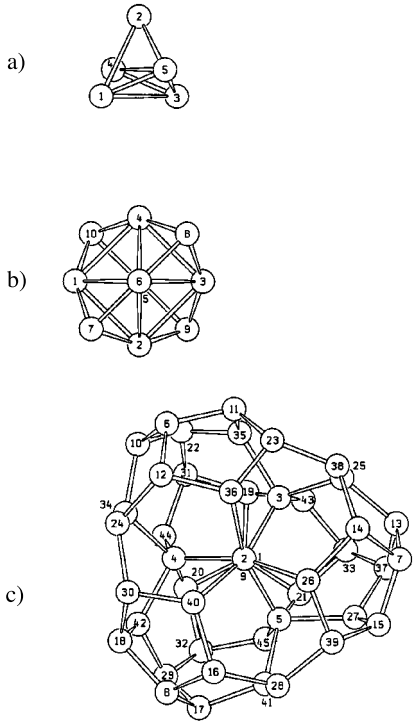

Figure 6.

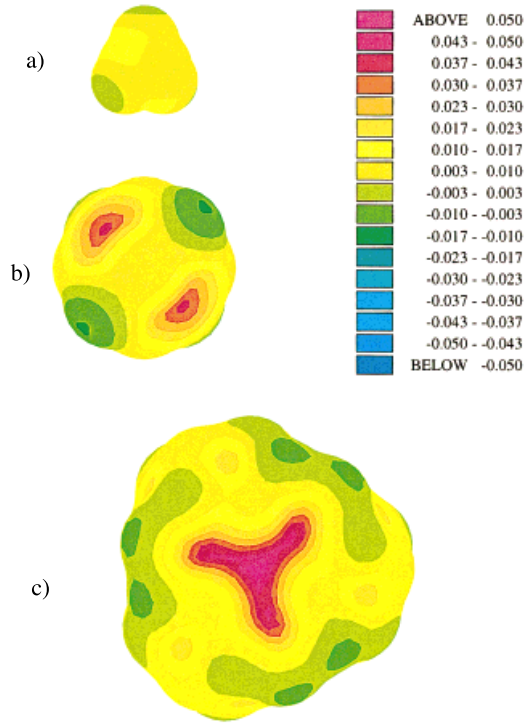

Figure 7.

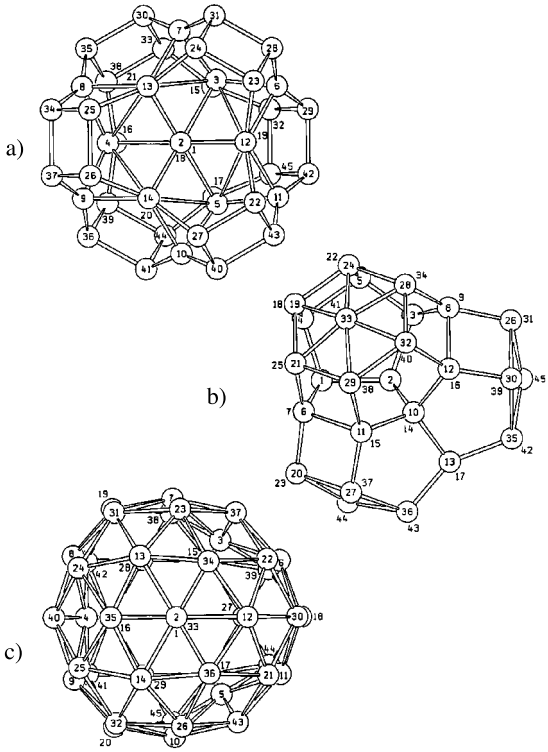

Figure 8.

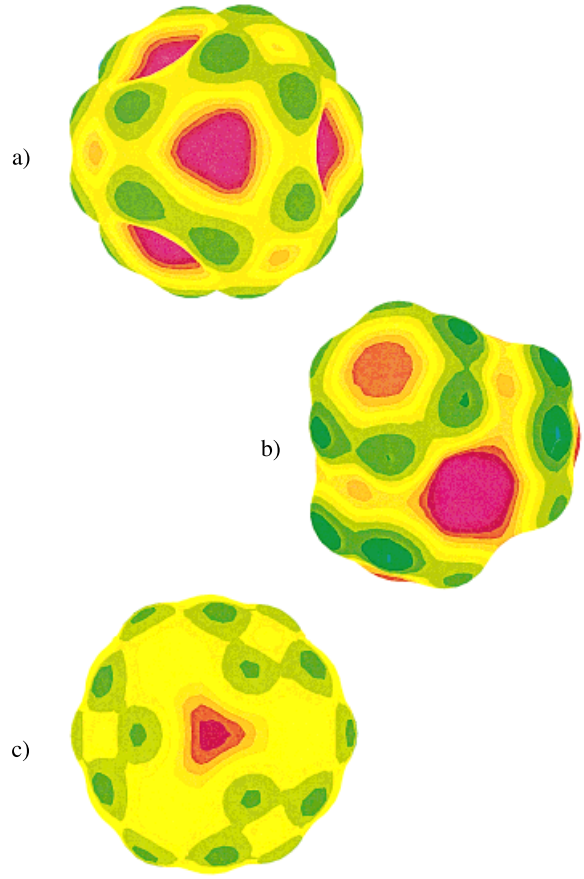

Figure 9.

with experiments, it must be considered that the measurements were done for cluster ions, whereas the calculations are for neutral systems.

Acknowledgments

This work was partially supported by Fonds der Chemischen Industrie. M. K. thanks C. Kölle for the program which generated the isodensity surfaces with the marching cube algorithm. The structures were drawn with the program SCHAKAL. The color plots of the MESP were generated with the program UNIRAS and the calculations were performed at the Siemens-Nixdorf S400/40 at RRZN Hannover.

References

1. B. G. Johnson, P. M. W. Gill, J. A. Pople, and D. J. Fox, *Chem. Phys. Lett.*, **206**, 239 (1993).
2. A. M. Köster, C. Kölle, and K. Jug, *J. Chem. Phys.*, **99**, 1224 (1993).
3. W.-P. Wang and R. G. Parr, *Phys. Rev. A*, **16**, 891 (1977).
4. W. A. Sokalski and R. A. Poirier, *Chem. Phys. Lett.*, **98**, 86 (1983).
5. W. A. Sokalski, M. Shibata, R. L. Ornstein, and R. Rein, *J. Comput. Chem.*, **13**, 883 (1992).
6. P. O. Löwdin, *J. Chem. Phys.*, **21**, 374 (1950).
7. D. N. Nanda and K. Jug, *Theor. Chim Acta*, **57**, 95 (1980).
8. K. Jug and D. N. Nanda, *Theor. Chim Acta*, **57**, 107, 131 (1980).
9. K. Jug, R. Iffert, and J. Schulz, *Int. J. Quant, Chem.*, **32**, 265 (1987).
10. J. Li, P. Correa de Mello and K. Jug, *J. Comput. Chem.*, **13**, 85 (1992).
11. G. Rauhut and T. Clark, *J. Comput. Chem.*, **14**, 503 (1993).
12. C. A. Reynolds, G. G. Ferenczy, and W. G. Richards, *J. Mol. Struct.* (*Theorem*), **256**, 249 (1992).
13. A. L. McClellan, *Tables of Experimental Dipole Moments*, Vol. 1, W. H. Freeman and Co., San Francisco and London, 1963.
14. A. L. McClellan, *Tables of Experimental Dipole Moments*, Vol. 2, Rahara Enterprises, El Cerrito, 1974.
15. M. J. Frisch, M. Head-Gordon, G. W. Trucks, J. B. Foresman, H. B. Schlegel, K. Raghavachari, M. Robb, J. S. Binkley, C. Gonzalez, D. J. Defrees, D. J. Fox, R. A. Whiteside, R. Seeger, C. F. Melius, J. Baker, R. L. Martin, L. R. Kahn, J. J. P. Stewart, S. Topiol, and J. A. Pople, *Gaussian 90, Revision F*, Gaussian, Inc., Pittsburgh PA, 1990.
16. M. Krack, K. Jug, *Chem. Phys.*, **192**, 127 (1995).
17. M. L. Connolly, *J. Appl. Cryst.*, **16**, 548 (1983).
18. B. Lee and F. M. Richards, *J. Mol. Biol.*, **55**, 379 (1971).
19. E. Silla, I. Tuñón, and J. L. Pascual-Ahuir, *J. Comput. Chem.*, **12**, 1077 (1991).
20. J. S. Murray and P. Politzer, *Theor. Chim. Acta*, **72**, 507 (1987).
21. T. Brinck, J. S. Murray, and P. Politzer, *Int. J. Quant. Chem.: Quant. Biol. Symp.*, **19**, 57 (1992).
22. R. F. W. Bader and H. J. T. Preston, *Theor. Chim. Acta*, **17**, 384 (1970).
23. W. E. Lorensen and H. E. Cline, *Comp. Graph.*, **21**, 163 (1987).
24. W. Heiden, T. Goetze, and J. Brickmann, *J. Comput. Chem.*, **14**, 246 (1993).
25. K. Jug and M. Krack, *Int. J. Quant. Chem.*, **44**, 517 (1992).
26. K. Raghavachari, *J. Chem. Phys.*, **84**, 5672 (1986).
27. K. Raghavachari and C. M. Rohlfing, *J. Chem. Phys.*, **89**, 2219 (1988).
28. J. L. Elkind, J. M. Alford, F. D. Weiss, R. T. Laaksonen, and R. E. Smalley, *J. Chem. Phys.*, **87**, 2397 (1987).
29. J. M. Alford, R. T. Laaksonen, and R. E. Smalley, *J. Chem. Phys.*, **94**, 2618 (1991).
30. K. Jug and M. Krack, *Chem. Phys.*, **173**, 439 (1993).
31. E. Kaxiras, *Chem. Phys. Lett.*, **163**, 323 (1989).
32. C. H. Patterson and R. P. Messmer, *Phys. Rev. B*, **42**, 7530 (1990).
33. D. A. Jelski, B. L. Swift, T. T. Rantala, X. Xia, and T. F. George, *J. Chem. Phys.*, **95**, 8552 (1991).